

Thermo-Elastic-Plastic Analysis on Internal Processing Phenomena of Single-Crystal Silicon by Nanosecond Laser

Takeshi MONODANE*, Etsuji OHMURA*, Fumitsugu FUKUYO**,
Kenshi FUKUMITSU**, Hideki MORITA** and Yoshinori HIRATA**

*Div. materials and Manufacturing Science, Osaka University, 2-1, Yamada-Oka, Suita, Osaka, Japan

E-mail: monodane@mapse.eng.osaka-u.ac.jp

**Hamamatsu Photonics K.K., 314-5, Shimo-Kanzo, Iwata, Shizuoka, Japan

When a nanosecond pulse laser is irradiated into a single crystal silicon, a local area near the focal point is melted and solidified, and internal cracks develop from this modified layer to the surrounding single crystal layer. This processing is applied to a dicing of silicon wafer, which is called stealth dicing (SD) and attracts attention in industries of semiconductor. A light of 1064 nm penetrates usually through a single crystal silicon. When a pulsed laser of this wavelength with high pulse energy is focused up to near the diffraction limit inside the silicon, however, strong absorption occurs near the focal point. This phenomenon depends on not only increase of beam intensity by focusing but also the temperature dependence of absorption coefficient. We conducted the thermo-elastic-plastic analysis by the finite element method, and calculated the stress intensity factor. As a result, the stress intensity factor exceeds the fracture toughness of a silicon. This result suggests the possibility of crack development from the modified layer to the surrounding single crystal layer.

Keywords: laser dicing, silicon, nanosecond laser, internal processing, absorption coefficient

1. Introduction

When a permeable nanosecond pulse laser is focused into a single crystal silicon, a polycrystalline region is formed at the neighborhood of focal point. A silicon wafer which has internal modified layer can be separated into individual chip easily by applying tensile stress. This processing is used for dicing of silicon wafer, which is called "Stealth Dicing (SD)" and attracts attention in the industries of semiconductor [1, 2]. Schematic of SD processing is shown in Fig. 1. A permeable pulse laser is focused into a silicon wafer and scanned in the horizontal direction. As a result, SD layer (hereinafter referred to as modified layer) is formed. A silicon wafer can be separated along the line of this layer because many internal cracks are developed from this layer. Figure 2 shows a cross section of silicon separated by the SD processing. Laser pulses were irradiated from top to down of the picture. The belt-shaped zone shows a modified layer. Cracks develop to the upper and lower sides from this layer. In the Stealth Dicing, a perme-

able laser is adopted and a silicon wafer is separated by inner processing. Therefore there is no damage at the surface layer of a wafer. Moreover there is no chipping, no cut loss and much smaller heat affected zone compared with other dicing technologies.

However, the mechanism of the internal processing phenomenon such as local polycrystallization and internal crack generation has not been clarified. It is known generally that very large thermal stress is generated when a laser absorption is induced locally in a short time. Therefore, purpose of this study is to clarify the mechanism of this phenomenon from the standpoint of the thermal stress. First, internal temperature rise of a silicon was calculated when a permeable laser of 1064 nm is irradiated. Second, stress distribution during laser irradiation was analyzed by the finite element method. Last, based on the obtained thermal stress distribution, progress of an internal crack was investigated by the stress intensity factor assuming that

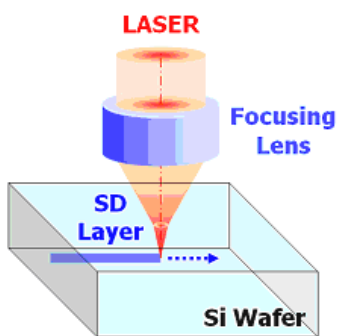


Fig. 1 Schematic of Stealth Dicing

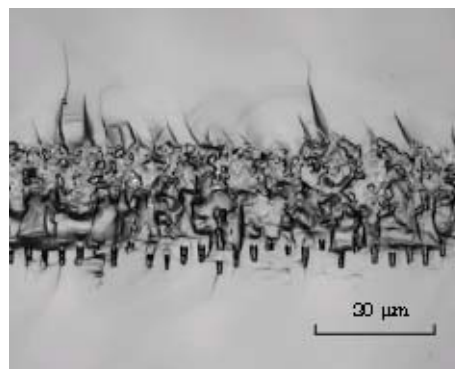


Fig. 2 SEM image of cross section divided by Stealth Dicing processing

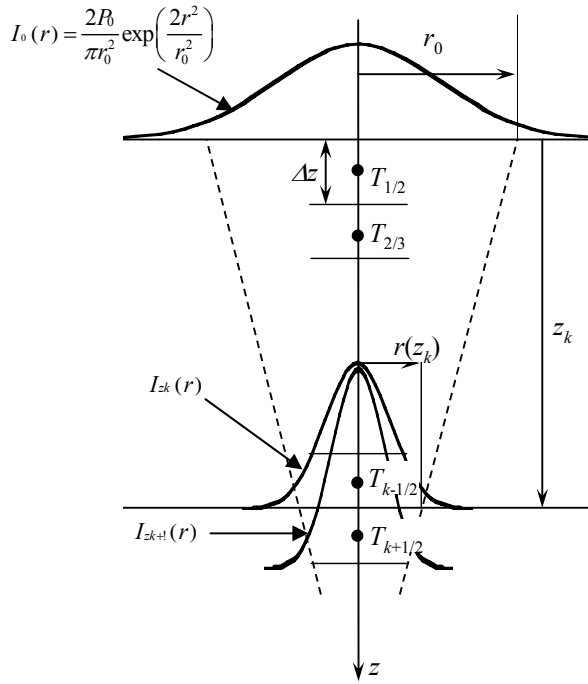


Fig. 3 Beam focusing model

Table 1 Laser irradiation condition for analysis

Wavelength	1064 nm
1/e ² radius	0.485 μm
Pulse duration	150 ns
Pulse shape	Isosceles triangle

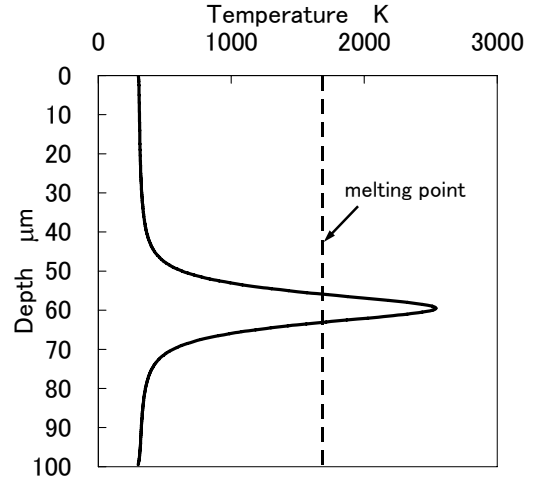


Fig. 4 Temperature rise of silicon along center line of beam calculated with absorption coefficient at room temperature

initial cracks exist in modified layer.

2. Calculation of temperature rise in Si

In order to calculate the maximum temperature rise in Si, we paid attention to the temperature rise only along the central axis of laser beam. The temperature rise was calculated simply without considering the thermal diffusion.

2.1 Method of analysis

Beam focusing model is shown in Fig. 3. Considering that a laser beam is axisymmetric, the cylindrical coordinate system O-rz was introduced. In this coordinate system, z-axis is taken along the central axis of laser beam and r-axis is taken in the radial direction.

As shown in Fig. 3, the depth was separated by a small depth Δz. The depth kΔz is denoted by z_k. The 1/e² radius at the depth z_k is denoted by r(z_k). T_{k-1/2} is the mean temperature between the depths z_{k-1} and z_k. An absorption coefficient considering temperature dependence is denoted by α(T). When Lambert law is applied between the depths z_{k-1} and z_k, the intensity I_k at the depth z_k is expressed by

$$I_k = I_{k-1} \exp[-\alpha(T_{k-1/2})\Delta z] \left(\frac{r_k}{r_{k+1}}\right)^2, \quad k = 0, 1, 2, \dots, k_{max} \quad (1)$$

where focusing or divergence of a beam can be evaluated by (r_k / r_{k+1})². When the laser power on the surface is P₀, the intensity distribution in the radial direction I₀(r) on the surface (k = 0) is given by

$$I_0(r) = \frac{2P_0}{\pi r_0^2} \exp\left(-\frac{2r^2}{r_0^2}\right) \quad (2)$$

Substituting Eq. (2) into Eq. (1), Eq. (1) can be expressed by

$$I_k = \frac{2P_0}{\pi r_0^2} \exp\left[-\sum_{i=0}^k \alpha(T_{i-1/2})\Delta z\right] \quad (3)$$

Internal heat generation per unit volume in the small interval (z_k, z_{k+1}) is given by

$$w_{k+1/2} = \frac{I_k - I_{k+1}}{\Delta z} = \frac{2P_0}{\pi r_0^2 \Delta z} \exp\left[-\Delta z \sum_{i=0}^k \alpha(T_{i-1/2})\right] \{1 - \exp[-\Delta z \alpha(T_{k+1/2})]\} \quad (4)$$

Therefore, the temperature rise in the small section along the central axis during Δt is evaluated by

$$\Delta T_{k+1/2} = \frac{w_{k+1/2} \Delta t}{\rho c} \quad (5)$$

where ρc is the heat capacity per unit volume.

2.2 Calculation Result

Concrete analysis was conducted under the irradiation condition shown in Table 1. Pulse energy E_p is effective value to penetrate silicon. It was supposed that the thickness of single crystal silicon is 100 μm, the depth of focal point is 60 μm and the initial temperature is 293 K. The physical properties of single-crystal silicon were referred to Refs. [3-5].

For the comparison, the temperature rise was calculated when the absorption coefficient is 7.87 1/cm [3], which is a value at room temperature. Calculation result of the maximum temperature rise is shown in Fig.4. The area whose temperature reaches melting point is only the range of 5 to 6 μm near the focal point. The melted area must be smaller if thermal diffusion is considered. On the other hand, the width of modified layer is about 20 μm as shown in Fig. 2. It can be supposed that much more intense laser absorption was induced actually. Therefore, the temperature rise was calculated considering the temperature dependence of absorption coefficient of single crystal silicon for 1064 nm

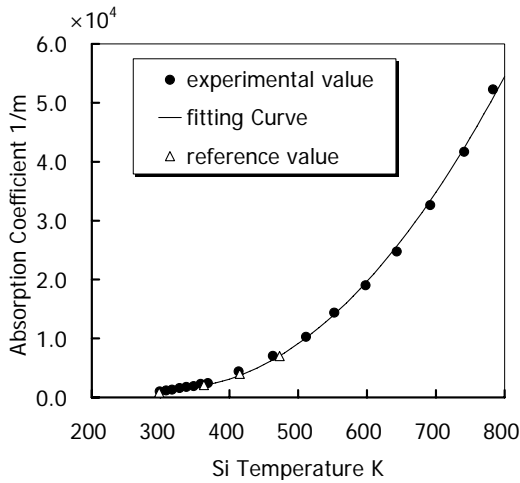


Fig. 5 Temperature dependence of absorption coefficient of silicon for 1064 nm [6,7]

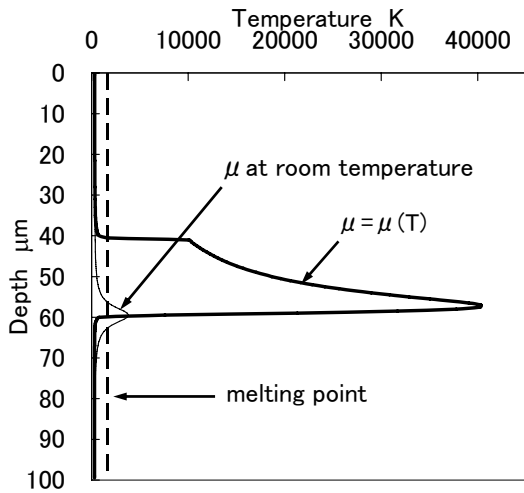


Fig. 6 Comparison of temperature rise along center line of beam between two different models

shown in Fig. 5. In Fig. 5, the experimental values by Fukuyo et al. were measured below 800 K. The values at more than 800 K were extrapolated from experimental data. The absorption coefficient of fused silicon is 7.61×10^5 1/cm [8].

Calculation result is shown in Fig. 6. Comparing with Fig. 4, much more intense laser absorption is induced. Especially, high temperature area is located between the depth 60 μm and 40 μm. Temperature becomes the maximum at the depth 58 μm and the temperature distribution is not symmetric with respect to the focal plane. Laser absorption begins at the focal point where the laser intensity is highest, and temperature rises suddenly. Once the temperature rises, temperature rises gradually also at the depth which is shallower than the focal point with increase of laser intensity and absorption coefficient. On the other hand, the temperature hardly rises below the focal point. Because the laser beam has been absorbed up to the focal point, therefore the laser intensity falls abruptly below the focal point. It can be considered that the internal processing phenomenon shown in Fig. 2 was caused by the temperature dependence of absorption coefficient.

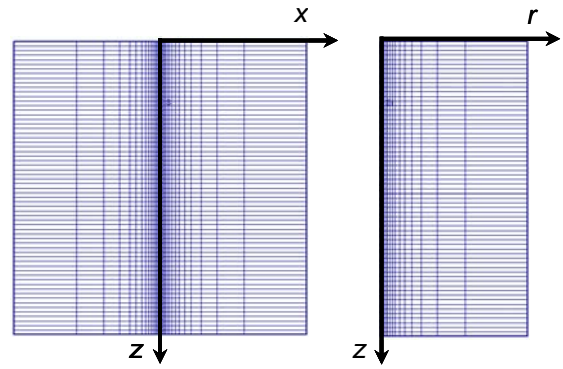


Fig. 7 Analysis model for stress distribution

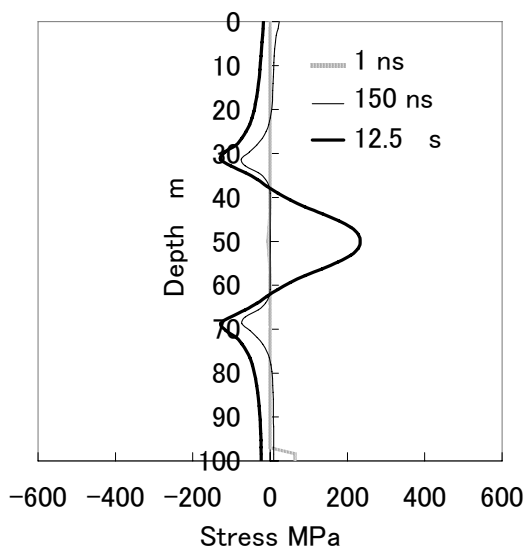
3. Thermo-elastic-plastic analysis by FEM

3.1 Method of analysis

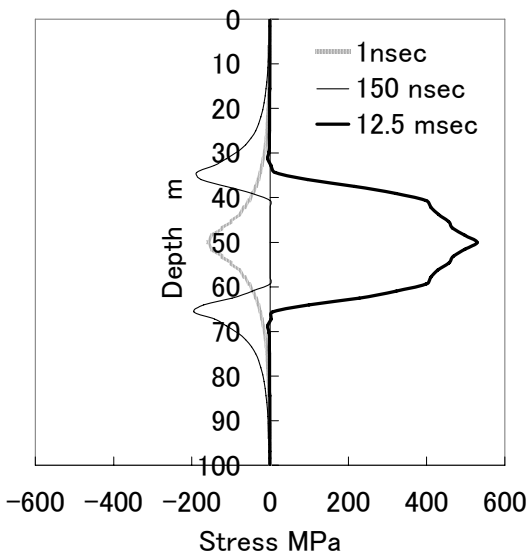
The stress distribution of the inside of silicon was analyzed by the finite element method.

As an analysis model, the plane strain model and axisymmetric model were examined. In both models, four-node quadrilateral element was used as shown in Fig.7. The analysis domain of the plane strain model was 100 μm in width and 100 μm in height, and the number of elements was 2304 and the number of nodes was 2405. The analysis domain of the axisymmetric model was 50 μm in radius and 100 μm in height, and the number of elements was 1152 and the number of nodes was 1235. The axis of symmetry corresponds to the central axis of the beam. The temperature and the stress distributions were calculated for both models when the laser is focused at the center of the analysis domain.

The heat source was given by the laser absorption whose peak was taken at the focal point. It was supposed that the heat source distribution is Gaussian in the radial direction and damps in the depth direction symmetrically according to the law of Lambert Beer. The absorption coefficient used 1×10^3 1/cm, which is the value at 1000 K that was extrapolated from the measurement results shown in Fig. 5. 1000 K is almost the average temperature between room temperature and melting point. The heat input was given so that the temperature at the area of 20 μm between depth 40 μm and 60 μm exceeds the melting point of silicon. Concretely, the heat input in the plane strain model was 0.36 μJ, and that in the axisymmetric model was 1.2 μJ. Heat diffuses three-dimensionally in the axisymmetric model, on the other hand, heat diffuses two-dimensionally in the plane model. Therefore, the heat input is different between these two models. It was supposed that the pulse width is 150 ns and the pulse shape is an isosceles triangle. The side and the bottom of the analysis domain were fixed and the upper surface was not restricted and the all surfaces were insulated. The physical properties of the single-crystal silicon were referred to Refs. [3-5] and [9] and their temperature dependence was considered.



(a) Distribution of σ_{xx} in plane strain model



(b) Distribution of σ_{rr} in axisymmetric model

Fig. 8 σ_{xx} and σ_{rr} distributions along center line of beam

3.2 Calculation result and discussion

Distributions of the vertical stress σ_{xx} and σ_{rr} along the central axis of the beam at several times are shown in Fig. 8. In this figure, negative stress shows compression, and positive value shows the tensile stress. At 1 ns which is just after the beginning of laser irradiation, compressive stress is generated near the focal point in both models. At this time, the area near the focal point is heated, but surrounding area is kept at low temperature. Therefore, the area near the focal point is immobilized by the surrounding area. At 150 ns, the inside temperature reaches maximum. Especially, the temperature near the focal point exceeds the melting point. Therefore, stress hardly acts near a focal point. This time is just after the end of laser pulse. At 12.5 μ s, very strong tensile stress is generated near the focal point. At this time, the inside of silicon is cooled off to the room temperature. The area where the tensile stress acts is the area where the compressive stress exceeded the yield-

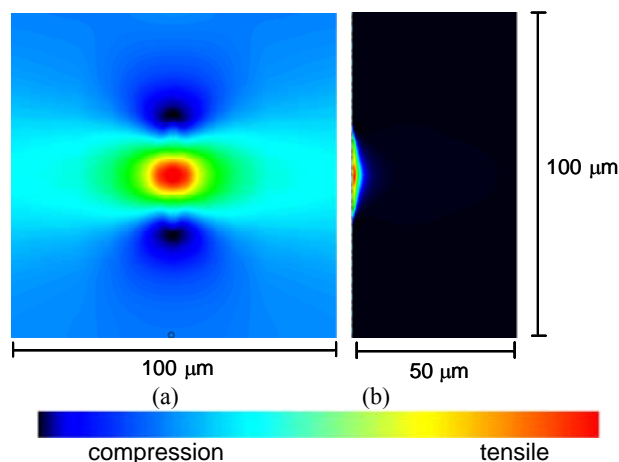


Fig. 9 (a) Distribution of σ_{xx} at 12.5 μ s analyzed with two-dimensional plane stress model. (b) Distribution of σ_{rr} at 12.5 μ s analyzed with two-dimensional axisymmetric model

ing point during heating process and plastic deformation occurred. In the plane strain model, the maximum compression is -128.96 MPa, and the tensile stress is 233.13 MPa. Both of them is at 12.5 μ s. Meanwhile, in the axisymmetric model, the maximum compression and the tensile stress are -194.71 MPa at 150 ns and 528.8 MPa at 12.5 μ s respectively.

The distribution of σ_{xx} and σ_{rr} of the both models at 12.5 μ s is shown in Fig. 9 by color scale. The restriction around the heat source is different between two models. Therefore, the stress distribution around the focal point is also different. Nevertheless tensile stress is generated near the focal point in both models. When laser is irradiated into a silicon and a local area is melted, strong tensile stress is generated in the heated area after cooling. The area where tensile stress acts corresponds to the polycrystalline area of the cross sectional picture shown in Fig. 2. When tensile stress acts on grain boundaries, there is a possibility that cracks develop in a silicon.

3.3 Calculation of the stress intensity factor

The stress intensity factor was calculated when the previous strong tensile stress is applied on the assumption that an initial crack exists in the inside of silicon. Calculation model is shown in Fig. 10. A Griffith crack of various length was assumed along the central axis of a beam. Only the mode one was examined because it is expected that the crack propagates in the vertical direction here. The stress intensity factor in the upper end and lower end of a crack can be calculated by Eq. (7).

$$K_{I\pm a} = \frac{2}{\sqrt{\pi a}} \int_{-a}^a \sqrt{\frac{a \pm \xi}{a m \xi}} \sigma_o(\xi) d\xi \tag{7}$$

Originally, Eq. (7) should be applied to the two dimensional plane model. In this study, it is overestimated but Eq. (7) was applied to also the axisymmetric model, assuming that an internal crack exists along the central axis and the stress acts perpendicularly to a crack.

The analysis result at 12.5 μ s which is obtained in the previous section was substituted into $\sigma_o(\xi)$ in Eq. (7). The calculation results in both models are shown in Fig. 11. According to Ref. [9], the fracture toughness of a polycrys-

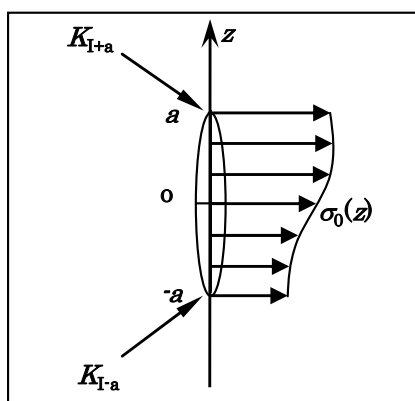


Fig. 10 Analysis model of stress intensity factor

talline silicon is about $0.6 \text{ MPa}\sqrt{\text{m}}$. The stress intensity factor exceeded the fracture toughness in the both models, therefore it is considered that internal cracks develop from the polycrystalline layer. On the other hand, in the axisymmetric model, the stress intensity factor exceeded the fracture toughness of a single crystal silicon which is $1.2 \text{ MPa}\sqrt{\text{m}}$ [10]. In the actual processing, the heat source can be regarded axisymmetric. Therefore, the analysis result of the stress distribution in the axisymmetric model reflects better the actual processing phenomenon than that in the plane strain model. As above mentioned, the stress intensity factor calculated in the axisymmetric model is overestimated. Therefore, in SD processing, it is concluded that the stress intensity factor by the thermal stress exceeds enough at least the fracture toughness of a polycrystalline silicon. There is a possibility that the stress intensity factor exceeds also the fracture toughness of a single crystal silicon.

4. Conclusion

The following conclusions were obtained by thermoelastic-plastic analysis of the single crystal silicon in SD processing.

(1) Local laser absorption is induced in the vicinity of a focal point because of the temperature dependence of absorption coefficient. Only the neighborhood of a focal point is heated and reaches higher temperature than the melting point. After rapid cooling, a strong tensile stress is generated in the vicinity of a focal point.

(2) When the stress intensity factor was calculated from the stress distribution after enough cooling, it exceeded the fracture toughness of a polycrystalline silicon. Therefore, the possibility was shown that the grain boundary does the role of an initial crack and the cracks develop from the polycrystalline layer.

References

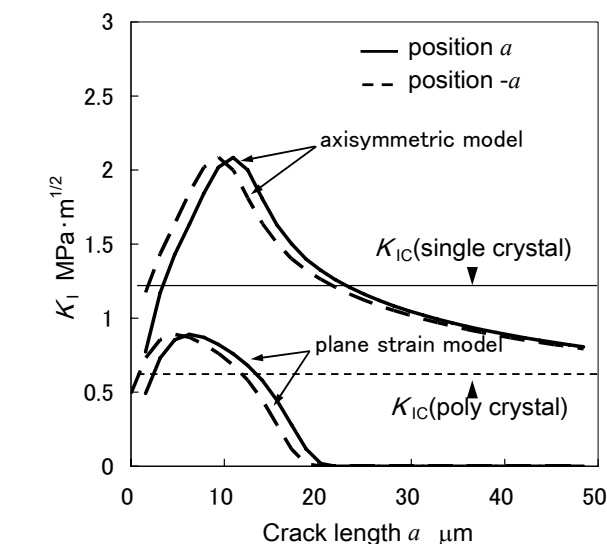


Fig. 11 Stress intensity factor calculated by two different models

- [1] Fukuyo, F.: The Stealth Dicing Technologies and Their Application, Jpn Laser Processing Soc, **12-1**(2005) 17. (in Japanese)
- [2] Fukuyo, F., Fukumitsu, K. and Uchiyama, N.: The Stealth Dicing Technologies and Their Application, Proc. of 6th LPM 2005, (2005).
- [3] Palik, E.D.: Handbook of Optical Constants of Solids, Academic Press, (1985), 547.
- [4] Touloukian, Y.S. ed.: Thermophysical Properties of Matter, **1**, TPRC, (1973), 878
- [5] Grabmaier, J.: Crystals Growth, Properties, and Applications, **5**, Springer-Verlag, (1979).
- [6] Fukuyo, F., Ohmura, E., Fukumitsu, K. and Morita, H.: Measurement of Temperature Dependences of Refractive Index and Absorption Coefficient of Single Crystal Silicon, Transactions of the Japan Society of Mechanical Engineers, Series B (in Japanese) (to be submitted)
- [7] Weakliem, H.A. and Redfield, D.: Temperature dependence of the optical properties of silicon, J. Appl. Phys., **50-3**, (1979), 1491.
- [8] Jellison, Jr. G.E., Measurements of the Optical Properties of Liquid Silicon and Germanium Using Nanosecond Time-Resolved Ellipsometry, Applied Physics Letters, **51-5**(1987), 775.
- [9] Patel, J.R. and Chaudhuri, A.R.: Macroscopic Plastic Properties of Dislocation-Free Germanium and Other Semiconductor Crystals, I. Yield Behavior, J. Appl. Phys., **34-9**, (1963), 2778.
- [10] Li, X.P., Kasai, T., Nakao, S., Ando, T., Shikida, M., Sato, K. and Tanaka, H.: Anisotropy in fracture of single crystal silicon film characterized under uniaxial tensile condition, Sensors and Actuators, **117-1**, (2005), 143

(Received: June 7, 2006, Accepted: November 20, 2006)